http://dx.doi.org/10.5012/bkcs.2012.33.11.3767

The Effect of SiO_2 Shell on the Suppression of Photocatalytic Activity of TiO_2 and ZnO Nanoparticles

Min Hee Lee,[a] Umakant Mahadev Patil,[†,a] Saji Thomas Kochuveedu,[†] Choon Soo Lee, and Dong Ha Kim[†,*]

Automotive/Research & Develpment Division, Hyundai Mortor Group, Gyeonggi-do 445-706, Korea
[†]Department of Chemistry and Nano Science, Division of Molecular and Life Sciences, College of Natural Sciences, Ewha Womans University, Seoul 120-750, Korea. [*]E-mail: dhkim@ewha.ac.kr
Received August 4, 2012, Accepted August 26, 2012

In this study, we investigate the potential use of TiO_2@SiO_2 and ZnO@SiO_2 core/shell nanoparticles (NPs) as effective UV shielding agent. In the typical synthesis, SiO_2 was coated over different types of TiO_2 (anatase and rutile) and ZnO by sol-gel method. The synthesized TiO_2@SiO_2 and ZnO@SiO_2 NPs were characterized by UV-Vis, XRD, SEM and TEM. The UV-vis absorbance and transmittance spectra of core@shell NPs showed an efficient blocking effect in the UV region and more than 90% transmittance in the visible region. XRD and SAED studies confirmed the formation of amorphous SiO_2 coated over the TiO_2 and ZnO NPs. The FESEM and TEM images shows that coating of SiO_2 over the surface of anatase, rutile TiO_2 and ZnO NPs resulted in the increase in particle size by ~30 nm. In order to study the UV light shielding capability of the samples, photocatalytic degradation of methylene blue dye on TiO_2@SiO_2 and ZnO@SiO_2 NPs was performed. Photocatalytic activity for both types of TiO_2 NPs was partially suppressed. In comparison, the photocatalytic activity of ZnO almost vanished after the SiO_2 coating.

Key Words : TiO_2@SiO_2, ZnO@SiO_2, Sol-gel synthesis, Photocatalysis, UV-shielding agents

Introduction

For the past few years, increasing apprehension regarding ultraviolet (UV) radiation dosage received from the sun has pushed intensive studies on UV-blocking including both black light and dangerous radiation.[1-3] A relatively small increase in UV radiation has a substantial impact on human skin and eyes, the biosphere, and the production of ground-level ozone. Therefore, there is a need to develop alternative bulk transparent UV-shielding materials suitable for applications in UV-shielding windows, contact lenses, or glasses, *etc*.[2-4]

A few metal oxides have been widely used as an excellent UV absorber in outdoor textile and cosmetics products.[5] Compared with organic UV absorbers, for instance, TiO_2 and ZnO possess typical advantages of inorganic materials such as physical and chemical stability under both high temperature and UV irradiation, as well as low toxicity.[6-10] TiO_2 and ZnO nanoparticles (NPs) have received great attention because of their unique catalytic, electrical, gas sensing, and optical properties. Their non-toxicity, good electrical, optical, and piezoelectric behavior and other advantages such as their low cost and extensive applications in diverse areas are some of the reasons for this extensive attention.[5-10]

However, the application of TiO_2 and ZnO as a UV absorber is limited in many practical areas because of the inherent photocatalytic activity. For example, the photocatalysis results in color fading of fabrics and potential damage of the skin cells.[10-12] Hence, in order to utilize TiO_2 and ZnO NPs as UV absorbers in a safe and effective manner, it is of particular importance to develop efficient methods to reduce the photocatalytic activity of TiO_2 and ZnO. One of the approaches to the reduction of the photocatalytic activity of these materials is to build a non-conducting barrier, such as SiO_2, between metal oxides and the surrounding medium to prevent direct contact between them.[12,13] SiO_2-based composite nanospheres are of particular interest to many applications because of their biocompatibility, chemical stability and ease of surface modification with a wide range of functional groups.[14-18] By incorporating other types of materials, such as quantum dots or magnetic nanoparticles, the composite nanospheres can have multi-functionalized aspects. The SiO_2 shell can effectively block the photoactivity of the TiO_2 and ZnO nanoparticles *via* confinement of the photogenerated electron hole pairs because its valence and conduction band edges lie far lower and higher in energy than the respective counter parts of TiO_2 and ZnO.[19-21] Therefore, under intense UV irradiation for a long term, the silica coated TiO_2 and ZnO NPs may still retain excellent stability.

Although reverse micoemulsion technique is considered as one of the best methods to prepare well dispersed silica coated ZnO or TiO_2 nanocomposites, it requires expensive surfactants and additional purification steps to remove the surfactants and unreacted chemicals from the products. On the basis of the above discussion, we established a simple sol-gel protocol for the synthesis of convincingly well dispersed core@shell SiO_2-coated TiO_2 (anatase and rutile) and ZnO NPs, which does not demand extensive purification steps. To study the efficiency of SiO_2 coating, we compared their photocatalytic performance systematically.

[a]These authors contributed equally to this work.

Experimental

Reagents. All chemicals used in this work were obtained from the Sigma Aldrich Chemicals Co. Ltd. and are of analytical reagent grade. Tetraethylorthosilicate (TEOS), absolute ethanol, and aqueous ammonia solution (28 wt %) were purchased from Sigma Aldrich (Korea). TiO_2 (P25, 80% anatase, mean size of ~25 nm) and ZnO (BYK- 3840 Wrutzite, mean size of ~25 nm) was purchased from Degussa (Germany) and BYK (USA). All these reagents were used as received.

Synthesis of SiO_2-Coated TiO_2 and ZnO Nanoparticles. SiO_2 was coated onto the surface of TiO_2 and ZnO NPs in the following way. Rutile type TiO_2 NPs was prepared by heating anatase TiO_2 at 600 °C for 4 h in air. SiO_2 shell coating over TiO_2 and ZnO was achieved by a sol-gel method. In a typical sol-gel method, about 0.1 g of TiO_2 or ZnO NPs were dispersed into 30 mL ethanol and sonicated for 30 min. An appropriate amount (0.5 mL) of TEOS together with 20 mL of ethanol, 10 mL water and 0.5 mL aqueous ammonia solution was then added into colloidal solution. The mixture containing the TiO_2/ZnO, TEOS, solvent and aqueous ammonia solution was stirred for 2 h at room temperature. After 2 h, the precipitate was isolated by centrifuging and washed with ethanol and water several times. The as-obtained product was dried at 100 °C under vacuum for 2 h.

Characterization of Core@shell Nanoparticles. The crystal phase of the powder samples was analyzed using X-ray diffraction with Cu Kα radiation (D/max RA, Rigaku). The accelerating voltage and the applied current were 40 kV and 30 mA, respectively. The morphology of core@shell NPs was investigated using a JEOL JSM-6700F SEM microscope. TEM and SAED measurements were carried out on a JEOL JSM2100-F microscope operated at 100 kV. UV-vis absorbance spectra were obtained using a Sinco S-4100 spectrometer.

Photocatalytic Activities. In order to study the performance of photocatalytic activity of core@shell NPs, degradation of dye molecules was employed and monitored as model reaction. We prepared 10 ppm methylene blue (MB) solution by dissolving 10 mg powder in 1000 mL of distilled water. We mixed 2 mg of catalyst with 30 mL of MB in a quartz container and sonicated for 10 min to get a uniform dispersion. The samples were irradiated under stirring by a UV (Newport Co., model 66984) light source. UV-vis absorbance spectroscopy (Varian Cary 5000 UV-vis-NIR spectrophotometer) was used to record the change in absorbance maxima of the characteristic peaks of dye molecules.

Results and Discussion

XRD Analysis. The XRD spectra of bare and silica coated TiO_2 and ZnO NPs are shown in Figure 1. From Figure 1, a series of characteristic peaks of (a) anatase, (b) rutile TiO_2 and (c) wurtzite structure of ZnO NPs are observed and all peaks are in good agreement with the standard spectrum (JCPDS no.: 88-1175, 84-1286 and 89-7102). The peak

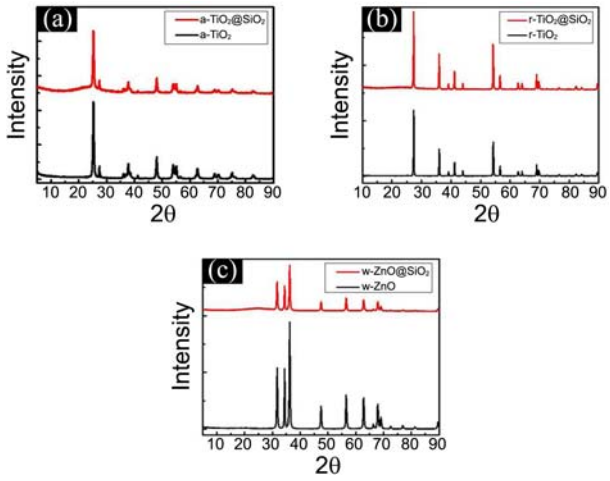

Figure 1. X-ray diffraction patters of (a) a-TiO_2 and a-TiO_2/SiO_2 (b) r-TiO_2 and r-TiO_2/SiO_2 (c) w-ZnO and w-ZnO@SiO_2 core@shell nanoparticles.

intensities of SiO_2 coated NPs are a little weaker than that of bare TiO_2 and ZnO NPs, which is possibly due to the presence of SiO_2 in an amorphous state around the NPs.[15] The degree of the reduction in intensity of characteristic peak of ZnO after SiO_2 coating is relatively higher than that of TiO_2, which may be due to the coating of thick layer of SiO_2 over ZnO as compared to TiO_2.

Optical Properties. Figure 2 shows UV-absorbance and

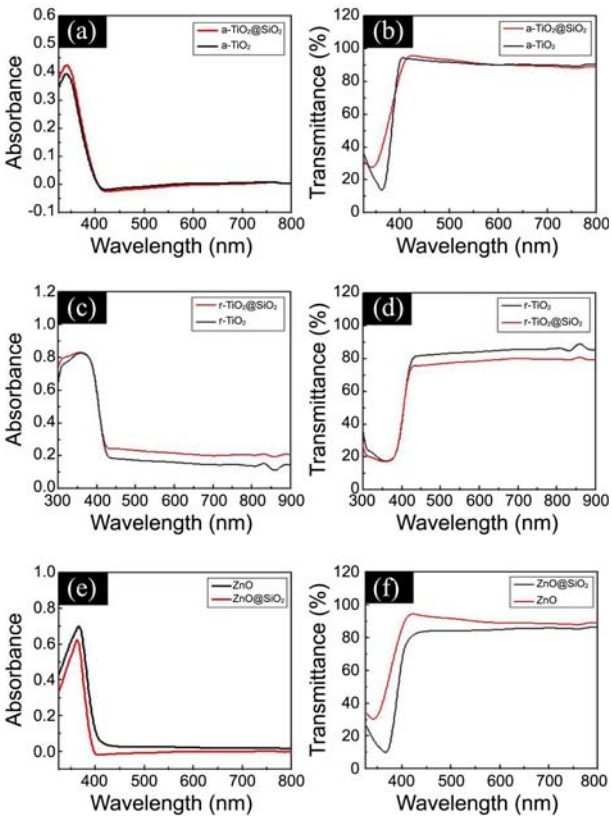

Figure 2. UV-vis absorption and transmission spectra of (a, b) a-TiO_2 and a-TiO_2/SiO_2 (c, d) r-TiO_2 and r-TiO_2/SiO_2 (e, f) w-ZnO and w-ZnO@SiO_2 core@shell nanoparticles.

transmittance spectra of bare and SiO_2 coated TiO_2 and ZnO composite nanoparticle suspensions. Anatase TiO_2 shows absorption at 400 nm (Fig. 2(a)) whereas rutile TiO_2 shows absorption edge up to 425 nm (Fig. 2(c)). Such a red shift in optical absorption observed in rutile TiO_2 may be due to an increase in particle size as a result of annealing and change in crystal structure. The bare ZnO (Fig. 2(e)) sample showed a sharp absorption onset at ~400 nm, which confirms that ZnO can block all UV region of solar spectrum. On the other hand, core@shell composite NPs did not show clear increase in absorption intensity due to the strong light scattering caused by the large particle size. Figure 2(b, d and f) shows transmission spectra of bare and SiO_2 coated anatase/rutile TiO_2 and ZnO NPs. All samples show absorption of UV light and excellent transmission in visible light (90%). Only a marginal loss in transmittance is observed in visible region after SiO_2 coating. It may be ascribed to the scattering of light subsequent to increase in particle size as a result of SiO_2 coating.[22,23]

Morphological Analysis. Figure 3(a-f) shows the FE-SEM images of bare and SiO_2 coated anatase, rutile TiO_2 and ZnO NPs. The anatase, rutile TiO_2 and ZnO NPs are basically of a sphere shape with mean diameter of ~25 nm as shown in Figure 3(a, c and e). Increase in particle size and smooth surface of the powder shown in Figure 3(b, d and f) confirms coating of SiO_2 shell over the surface. Figure 4(a-f) shows TEM images of bare and SiO_2 coated anatase, rutile TiO_2 and ZnO NPs. It is clearly seen that reasonably well dispersed core-shell nanoparticles without much aggregation is obtained. The TEM images show that the size of most of the bare TiO_2 and ZnO NPs is ~30 nm. Figure 4(b, d and f)

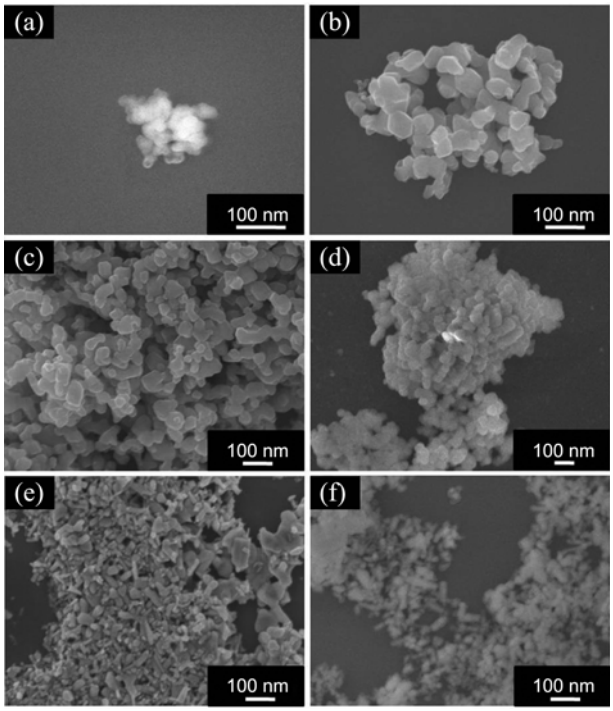

Figure 3. FESEM images of (a) a-TiO_2 (b) a-TiO_2/SiO_2, (c) r-TiO_2, (d) r-TiO_2/SiO_2, (e) w-ZnO, (f) w-ZnO@SiO_2 core@shell nanoparticles.

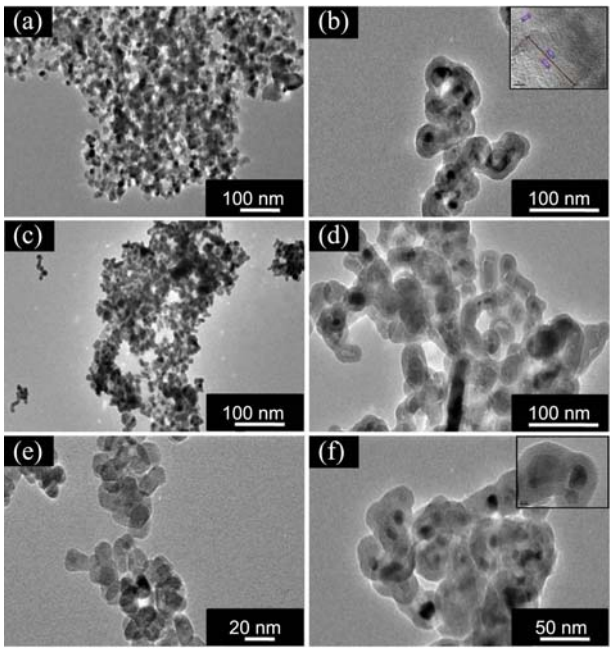

Figure 4. TEM images of (a) a-TiO_2 (b) a-TiO_2/SiO_2, (c) r-TiO_2, (d) r-TiO_2/SiO_2, (e) w-ZnO, (f) w-ZnO@SiO_2 core@shell nanoparticles.

shows the TEM images of the SiO_2 coated TiO_2 and ZnO NPs. From the TEM images of SiO_2 coated TiO_2 and ZnO in Figure 4(b, d and f), one can observe that the NPs are surrounded by some shades, implying the existence of SiO_2 shells and successful formation of the core/shell structures. The average diameter of TiO_2 and ZnO NPs are determined to be ~30 nm and the thickness of SiO_2 shell is estimated to be about ~25 nm. Inset of Figure 4(b and f) shows core@shell NPs of anatase TiO_2@SiO_2 and ZnO@SiO_2 at higher magnification, which proves that the shell thickness of SiO_2 is up to 25-30 nm. From the TEM image, one can see that thicker shell of SiO_2 was coated over the ZnO than over TiO_2 as shown in the inset of Figure 4(b and f). This result implies that the wurtzite type ZnO can offer more nucleation sites for the SiO_2 growth. The structure of the SiO_2 layer coated on the surface of TiO_2 and ZnO NPs was further investigated by the SAED pattern as shown in Figure 5. The diffraction patterns with circle of spots confirms the crystalline nature of TiO_2 and ZnO NPs. Broad and blurred ring observed in SAED pattern of SiO_2 coated particles confirms an amorphous nature of SiO_2 coating as shown in Figure 5(b, d).[24] The FESEM, TEM and SAED result confirm the formation of amorphous silica over the polycrystalline TiO_2 and ZnO NPs.

Photocatalytic Activity. Figure 6 shows the time-dependent absorption spectra of MB aqueous solutions during the UV light irradiation in the presence of bare and SiO_2 coated TiO_2 and ZnO composite NPs. For bare TiO_2 and ZnO NPs, the characteristic absorption peaks of UV decreased as the irradiation time increased and disappeared almost completely after irradiation for 300 min as shown in Figure 6(a, c and e). However, ~38% of MB was degraded onto the SiO_2

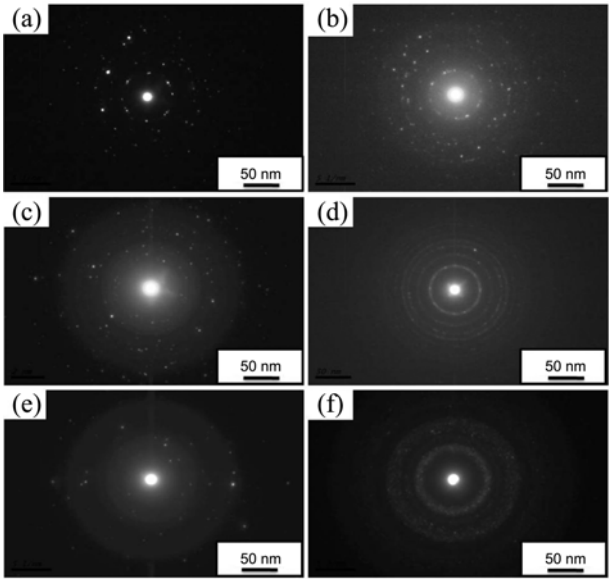

Figure 5. SAED patterns of (a) a-TiO_2 (b) a-TiO_2/SiO_2, (c) r-TiO_2, (d) r-TiO_2/SiO_2, (e) w-ZnO, (f) w-ZnO@SiO_2 core@shell nanoparticles. Insets in Figure 5(b) and (f) indicate magnified views of selected areas.

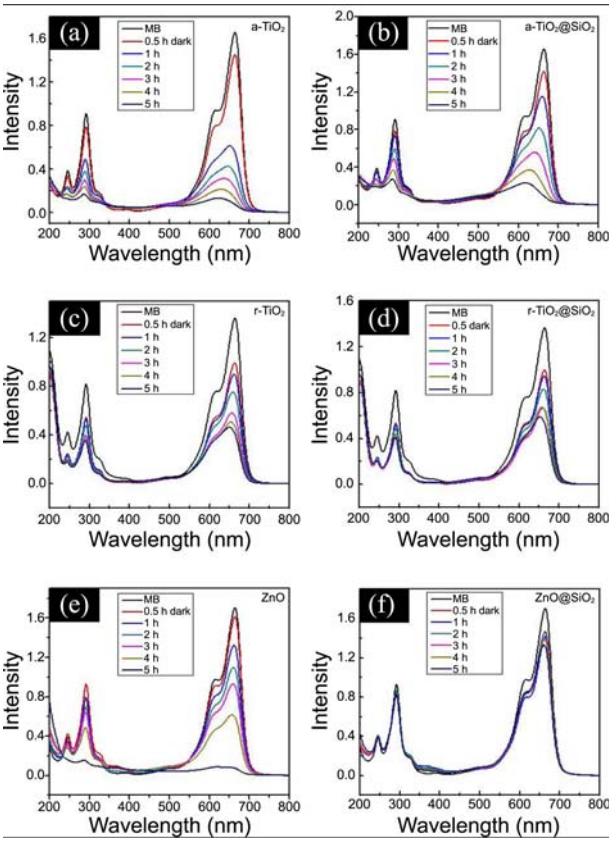

Figure 6. UV-vis absorption spectra for MB photocatalyzed by (a) a-TiO_2 (b) a-TiO_2/SiO_2, (c) r-TiO_2, (d) r-TiO_2/SiO_2, (e) w-ZnO, (f) w-ZnO@SiO_2 core@shell nanoparticles.

coated TiO_2 NPs compared with ~80% onto the neat TiO_2 for the same interval, while the SiO_2 coated ZnO showed only ~9% degradation of MB compared with neat ZnO NPs

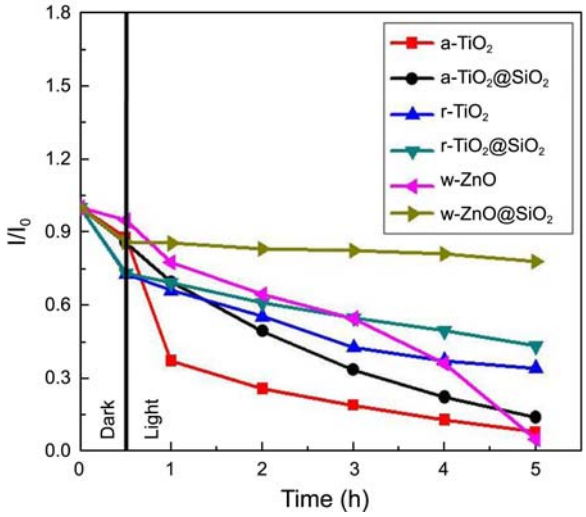

Figure 7. Relationship between C/C_0 and irradiation time for MB photocatalyzed by bare and SiO_2 coated TiO_2 and ZnO nanoparticles.

(~91%) as confirmed by Figure 6(b, d). In Figure 7, the overall photocatalytic performance was compared in terms of relationship between C/C_0 and irradiation time for MB photocatalyzed by bare and SiO_2 coated anatase/rutile-TiO_2 and ZnO NPs. Again, it is clearly confirmed that the SiO_2 coating led to a decrease in photocatalytic activity of TiO_2 and ZnO NPs. The difference in the degree of the suppression of photocatalytic activity of TiO_2@SiO_2 *vs.* ZnO@SiO_2 for MB degradation was measured to be ~50% (32% *vs* 82%), indicating that SiO_2 coating onto ZnO was more effective in decreasing the photocatalytic activity by almost 2 times than onto TiO_2. It is well known that rutile TiO_2 is much less photoactive than anatase TiO_2 in terms of photocatalytic efficiency,[25] and the difference in the activity between them was estimated to be up to ~10% in the current study. In summary, the coating of SiO_2 on the surface of ZnO NPs could markedly suppress the photodegradation of the MB solution under the irradiation of UV light.

Conclusion

In this study, moderately well dispersed TiO_2@SiO_2 and ZnO@SiO_2 composite NPs were successfully prepared using a simple sol-gel method. This method does not require any sophisticated reactants or any additional steps to purify the product unlike in the case of reverse microemulsion technique. The degree of dispersion or functionality of thus-obtained core@shell nanoparticles can be further modulated by modifying the silica surface using various organosilane compounds depending on target applications of interest. Optical absorption study shows SiO_2 coated TiO_2 and ZnO can absorb UV light with good transparency in visible region of solar spectrum. XRD and FESEM analysis revealed the successful coating of SiO_2 on TiO_2/ZnO surface. The core@shell structure has been confirmed by TEM images and SAED pattern. The SiO_2 coated TiO_2 and ZnO showed

distinctly reduced photocatalytic activity compared with neat TiO_2 and ZnO in terms of the degradation of MB by ~32% and ~82%, respectively. The nanocomposites consisting of ZnO core and thicker SiO_2 shell showed the most reduced photocatalytic properties and also have improved stability among the systems used in this study, suggesting that ZnO@SiO_2 type NPs are expected to act as potentially useful UV blocking agent.

Acknowledgments. This work was supported by the Hyundai NGV Project and the National Research Foundation (NRF) of Korea Grant funded by the Korean Government (20110029409).

References

1. Hoffmann, K.; Kaspar, K.; Gambichler, T.; Altmeyer, P. *J. Am. Acad. Dermatol*. **2000**, *43*, 1009.
2. Hatch, K. L. *Recent Res. Cancer Res*. **2002**, *160*, 42.
3. Zhang, Y.; Yu, L.; Ke, S.; Shen, B.; Meng, X.; Huang, H.; Fengzhu, L.; Xin, J. H.; Chan, H. L. W. *J. Sol-Gel Sci. Technol*. **2011**, *58*, 326.
4. Xin, J. H.; Daoud, W. A.; Kong, Y. Y. *Tex. Res. J*. **2004**, *74*, 97.
5. Daoud, W. A.; Xin, J. H.; Zhang, Y. H. *J. Non-Cryst. Solids* **2005**, *351*, 1486.
6. Daoud, W. A.; Xin, J. H.; Zhang, Y. H. *Surf. Sci*. **2005**, *599*, 69.
7. Fei, B.; Deng, Z.; Xin, J. H.; Zhang, Y. H.; Pang, G. *Nanotechnology* **2006**, *17*, 1927.
8. Huang, M. H.; Mao, S.; Feick, H.; Yan, H.; Wu, Y.; Kind, H.; Weber, E.; Russo, R.; Yang, P. *Science* **2001**, *292*, 1897.
9. Rodriguez, J. A.; Jirsak, T.; Dvorak, J.; Sambasivan, S.; Fischer, D. *J. Phys. Chem. B* **2000**, *104*, 319.
10. Wang, Y.; Li, X.; Lu, G.; Quan, X.; Chen, G. *J. Phys. Chem. C* **2008**, *112*, 7332.
11. Liu, C. H.; Zapien, J. A.; Yao, Y.; Meng, X. M.; Lee, C. S.; Fan, S. S.; Lifshitz, Y.; Lee, S. T. *Adv. Mater*. **2003**, *15*, 838.
12. Zhang, H.; Luo, X.; Xu, J.; Xiang, B.; Yu, D. *J. Phys. Chem. B* **2004**, *108*, 14866.
13. Lee, S. K.; Chung, K. W.; Kim, S. G. *Aerosol Sci. Tech*. **2002**, *36*, 763.
14. Hwang, S. T.; Hahn, Y. B.; Nahm, K. S.; Lee, Y. S. *Colloid Surface A* **2005**, *259*, 63.
15. Hu, Y.; Li, C.; Gu, F.; Zhao, Y. *J. Alloy Compd*. **2007**, *432*, L5.
16. Zhang, Y.; Wu, Y.; Chen, M.; Wu, L. *Colloid Surface A* **2010**, *353*, 216.
17. Ismail, A. A.; Ibrahim, I. A.; Ahmed, M. S.; Mohamed, R. M.; Elshall, H. *J. Photoch. Photobioy. A* **2004**, *163*, 445.
18. Lee, B. S.; Kang, D. J.; Kim, S. G. *J. Mater. Sci*. **2003**, *38*, 3545.
19. Liang, H. P.; Wan, L. J.; Bai, C. L.; Jiang, L. *J. Phys. Chem. B* **2005**, *109*, 7795.
20. Nann, T.; Mulvaney, P. *Angew. Chem. Int. Ed*. **2004**, *43*, 5393.
21. Chan, Y.; Zimmer, J. P.; Stroh, M.; Steckel, J. S.; Jain, R. K.; Bawendi, M. G. *Adv. Mater*. **2004**, *16*, 2092.
22. Li, F.; Huang, X.; Jiang, Y.; Liu, L.; Li, Z.; *Mat. Res. Bull*. **2009**, *44*, 437.
23. Wang, J.; Tsuzuki, T.; Sun, L.; Wang, X. *ACS Appl. Mater. Inter*. **2010**, *2*, 957.
24. Patil, U. M.; Gurav, K. V.; Joo, O.-S.; Lokhande, C. D. *J. Alloys and Comp*. **2009**, *478*, 711.
25. Sclafani, A.; Herrmann, J. M. *J. Phys. Chem*. **1996**, *100*, 13655.